PNAS
www.pnas.org

Supplementary Information for

First–in–Class Humanized FSH Blocking Antibody Targets Bone and Fat

Sakshi Gera, Damini Sant, Shozeb Haider, Funda Korkmaz, TanChun Kuo, Mehr Mathew, Helena Perez-Pena, Honglin Xie, Hao Chen, Rogerio Batista, Kejun Ma, Zhen Cheng, Elina Hadelia, Cemre Robinson, Anne Macdonald, Sari Miyashita, Anthony Williams, Gregory Jebian, Hirotaka Miyashita, Anisa Gumerova, Kseniia Ievleva, Pinar Smith, Jiahuan He, Vitaly Ryu, Victoria DeMambro, Matthew A. Quinn, Marcia Meseck, Se-Min Kim, T. Rajendra Kumar, Jameel Iqbal, Maria I. New, Daria Lizneva, Clifford J. Rosen, Aaron J. Hsueh, Tony Yuen, Mone Zaidi

Corresponding authors: Maria I. New (maria.new@mssm.edu) and Mone Zaidi (mone.zaidi@mssm.edu)

This PDF file includes:

Figures S1 to S5
Tables S1

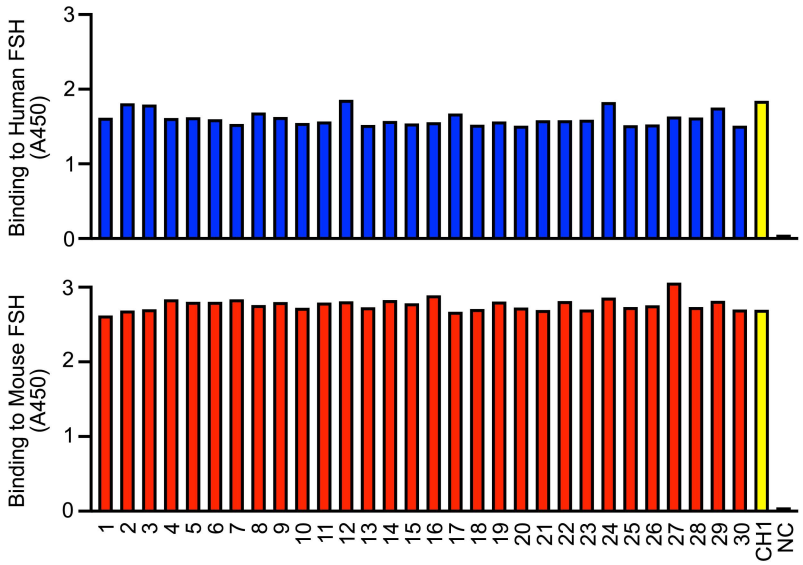

Figure S1: Confirmation of Binding of Humanized Antibody Clones to FSH. ELISA using plates coated with human (top panel) or mouse FSH (bottom panel). Binding was measured using HRP–conjugated mouse or human IgG after incubation of bacterial lysates from 30 humanized antibody clones (1-30) and the human–mouse chimera (CH1). NC – negative control without any IgG.

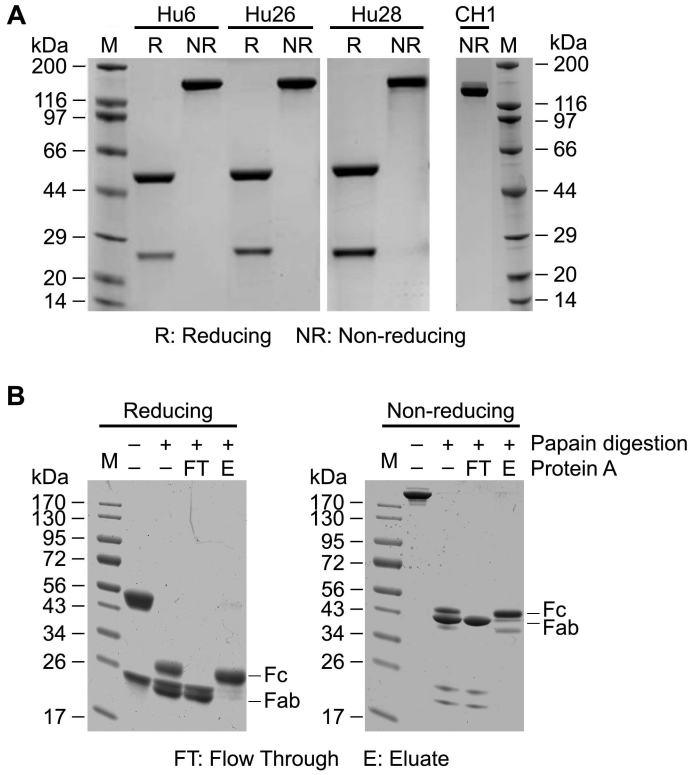

Figure S2: Purification of Selected Humanized Antibody Clones. SDS PAGE analysis of Hu6, Hu26, Hu28 and CH1 purified by protein A chromatography **(A)**, or following papain digestion **(B)**. Samples were loaded at 5 µg and were run under reducing (R) and non–reducing (NR) conditions.

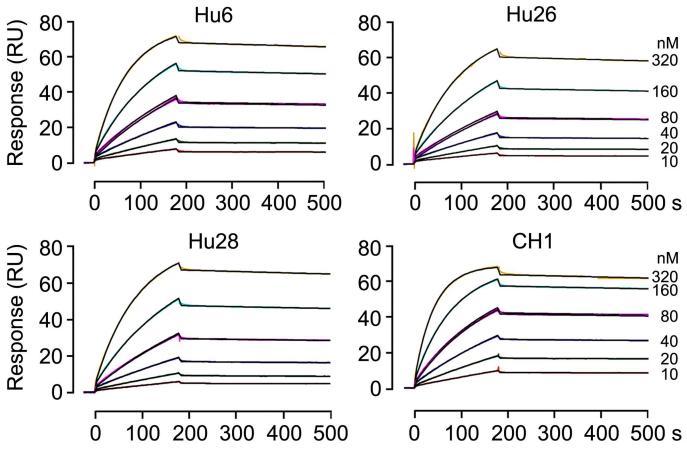

Figure S3: FSH–Blocking Antibodies Hu6, Hu26 and Hu28 Bind Mouse FSH. Sensograms from surface plasmon resonance measurements on Biacore 8K/T200 showing the concentration–dependent binding of humanized antibodies Hu6, Hu26 and Hu28 (10 – 320 nM) to mouse FSH. Please also refer to Fig. 1A and Table 1.

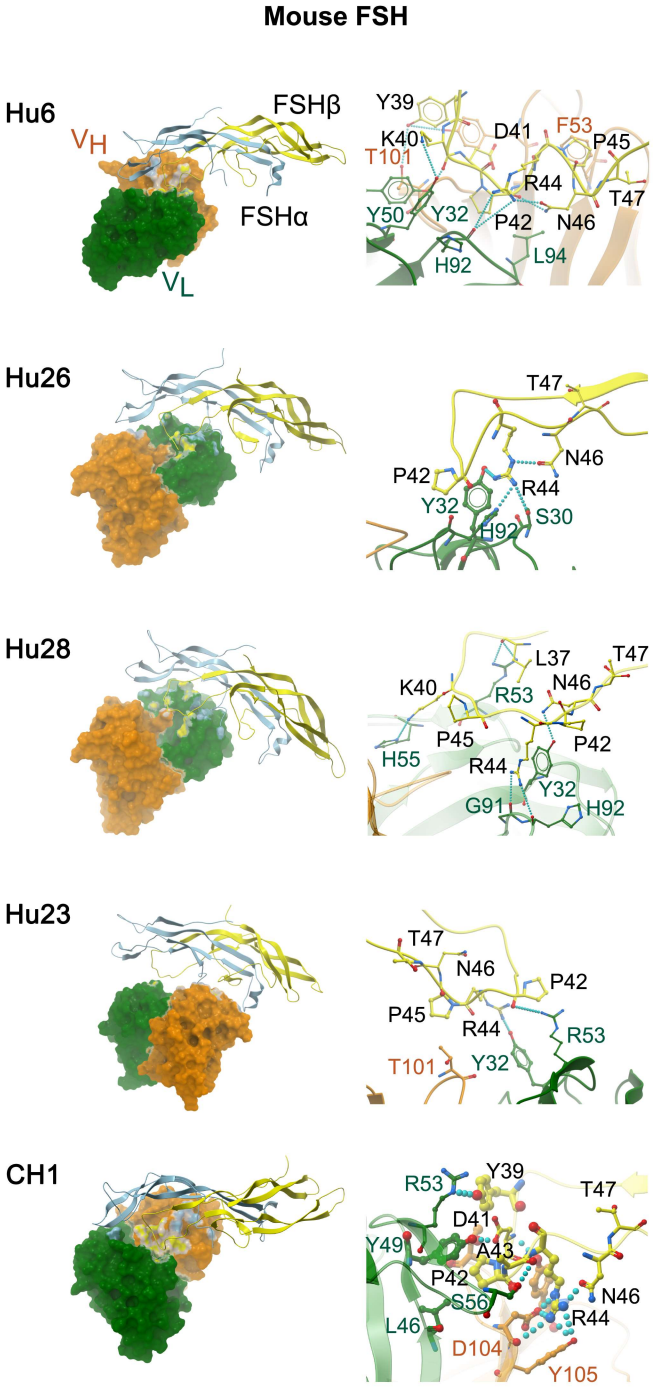

Figure S4: **Atom–Level Fine Mapping of Antibody–mouse FSH Interfaces.** Shown are computational models and fine maps of complexes between the α (blue) and β (yellow) subunits of mouse FSH, and the variable regions, V_L (green) and V_H (orange), of the humanized monoclonal antibodies Hu6, Hu26, Hu28 and Hu23, as well as the mouse-human chimeric antibody CH1. Interactions between specific amino acids are shown (Please also refer to Fig. 2A and Table 2).

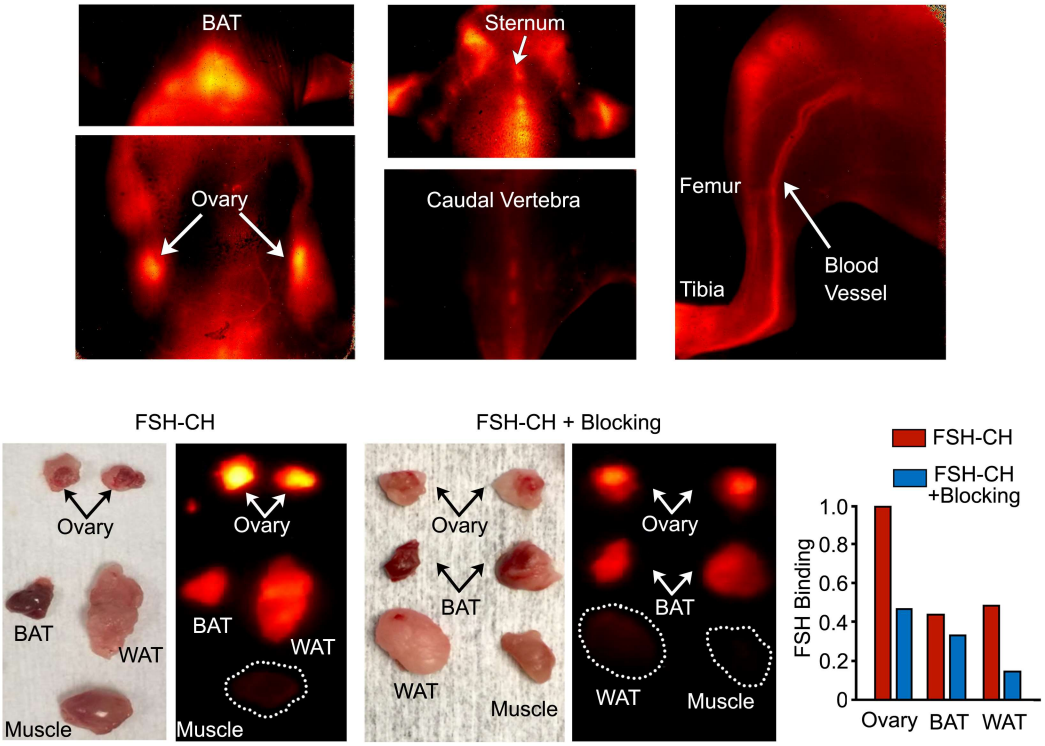

Figure S5: FSH Binding to White and Brown Adipose Tissue. NIR-II imaging of FSHR–expressing tissues 2 hours after injection of FSH-CH (12.5 μg) into the tail vein of mice. Signal in intact (top) and dissected tissues (bottom), namely ovaries, brown adipose tissues (BAT) and white adipose tissue (WAT). Attenuation of the NIR-II signal when FSH-CH was injected with a 30–fold molar excess of unconjugated FSH (bottom). Normalized fluorescence intensity for each tissue is also shown.

Anti-FSHβ Ab	K_a ($x10^4 M^{-1}s^{-1}$)	K_d ($x10^{-4}s^{-1}$)	K_D (nM)
Hu28	1.53	1.66	10.80
Hu6	1.00	2.14	21.40
Hu26	1.71	2.52	14.70
Hu14	1.35	3.03	22.40
Hu27	0.95	3.08	32.40
Hu12	0.17	3.22	191.00
Hu22	1.62	3.32	20.50
Hu4	1.41	3.34	23.70
CH2	2.39	3.88	16.20
Hu3	0.79	4.09	51.60
Hu5	0.77	4.38	56.90
Hu25	3.51	4.43	12.60
Hu30	3.37	4.54	13.50
Hu19	2.10	4.59	21.90
Hu20	1.35	4.65	34.40
Hu8	2.02	4.69	23.30
Hu24	0.98	5.13	52.50
Hu29	3.89	5.58	14.40
Hu18	1.57	5.62	35.80
Hu11	2.21	5.66	25.60
Hu16	1.66	5.71	34.30
Hu21	1.95	5.84	29.90
Hu2	2.21	5.98	27.00
Hu10	1.94	6.21	32.10
Hu13	0.05	7.76	1690.00
Hu9	3.24	8.26	25.50
Hu17	4.85	10.90	22.50
Hu1	5.29	12.00	22.70
CH1	5.54	12.70	23.00
Hu15	3.22	14.60	45.30
Hu23	3.02	21.80	72.30
Hu7	5.06	23.60	46.50

Table S1: FSH Binding to 30 Antibody–Expressing Bacterial Lysates. Surface plasmon resonance (SPR, Biacore) utilized to study the binding properties of human FSH with the crude bacterial lysates of 30 humanized clones of the anti–FSHβ antibody Hf2. These yielded measures of association constant (K_a), dissociation constant (K_d) and affinity (K_D). Clone 28, 6 and 26 displayed lowest K_d, and were thus chosen for purification and further characterization.